

Three-dimensional geological modelling of the eastern and western parts of the Hovsan field according to geological and geophysical data

T.R. Ahmedov, K.A. Kerimova, L.N. Khalilova, 2024

Azerbaijan State Oil and Industry University, Baku, Azerbaijan
Received 30 November 2023

The article considers the issue of volumetric modelling of productive formations of the Hovsan oil field using the PETREL software package.

The productive horizons QaS-2 and QaS-3 of the Qala Suite of the Productive Series in the eastern and western parts of the Hovsan field were taken as the object of the study. Geological and geophysical data for the research area were used to construct the model.

The Hovsan field is related to deposits of the Qala Suite in the western and eastern sections, separated by an industrially important oil-water zone. The deposits of the Qala Suite are divided into three horizons: (from top to bottom) QaS1 — 57 m, QaS2 — 70 m, and QaS3 — 168 m. The total thickness of the Qala Suite is 250 m in the western part and 280 m in the eastern part.

The article explains in detail the methodology for building 3D models of the eastern and western parts of the Hovsan field using both geological and well data for the research area. It also includes a petrophysical model of the eastern and western parts of the Hovsan field and a lithological cube for volumetric lithology modelling.

The paper shows that sands and sandstones (thickness 5—15 m), which are oil and gas reservoirs, are separated mainly in the upper and middle horizons, as well as in the top part of the lower layer of the lower horizon (thickness 30 m), which alternate with clay layers 2—3 m thick. The reservoir properties of the layers vary along the section and over the area.

Although the Hovsan field has been in production for more than 70 years, 3D geological and geophysical modelling was carried out for the first time for the eastern and western parts of the Qala Suite, which is considered promising in terms of productivity. For the first time, the research area was studied in detail from the point of view of lithology, petrophysics, and oil and gas content in the inter-well space using modelling based on 3D seismic data. On the other hand, 3D models are the basis for solving issues such as hydrocarbon resource estimation, justifying the drilling of new wells, monitoring resource development, and assessing the impact of waterflooding and production well operations. Using three-dimensional models made it possible to realise both long-term and operational forecasting when monitoring the exploitation of hydrocarbon fields.

Since the presence of new objects in the Qala Suite, considered promising in terms of productivity, is not in dispute, the study confirms their detection and monitoring with the application of three-dimensional models.

Key words: structural-parametric model, lithology cube, volumetric modelling, petrophysical modelling, reservoir, porosity, oil saturation.

Introduction. The Hovsan oil field was accumulated in the paleo-layer of the Qala Suite, and as a result of subsequent tectonic movements, the structure changed. In modern

Citation: *Ahmedov, T.R., Kerimova, K.A., & Khalilova, L.N. (2024). Three-dimensional geological modelling of the eastern and western parts of the Hovsan field according to geological and geophysical data. *Geofizychnyi Zhurnal*, 46(4), 134—148. <https://doi.org/10.24028/gj.v46i4.310473>.*

Publisher Subbotin Institute of Geophysics of the NAS of Ukraine, 2024. This is an open access article under the CC BY-NC-SA license (<https://creativecommons.org/licenses/by-nc-sa/4.0/>).

structural terms, it has become a monoclinical structure. The field is concentrated in the western and eastern parts of this monocline. It was found that one of the factors accelerating fluid movement in the layers is the energy of dissolved gases. The rapid decline in well flow rate at the field was caused by the extraction of dissolved gas together with oil during production. That is, dissolved gas and oil extraction caused a sharp drop in reservoir pressure.

The interaction of a long-term very rich hydrocarbon (combined with carbon dioxide and hydrogen sulphide) upward flow, which, judging by geochemical and geophysical (up to its manifestation in seismic sections) signs, continues even now, with various structures of the sedimentary cover and basement, which requires specification of the field model [Lukin, 2006]. In the Hovsan field, commercially significant oil-bearing potential is associated with deposits of the Qala Suite of the Productive Series in the western and eastern sections separated by a wet zone.

The deposits of the Qala Suite are divided into three horizons: (from top to bottom) QaS1 — 57 m, QaS2 — 70 m, and QaS3 — 168 m. The total thickness of the Qala Suite is 250 m in the western section and 280 m in the eastern section.

The subject of volumetric modelling of geological structure includes the shape of deposits (structural plan, morphology of fluid contact surface), internal structure of reservoir and deposits (spatial relationship of reservoirs and nonreservoirs, distribution of different types of fluids in the section), filtration-capacity properties of reservoir rocks and their oil and gas saturation [Kerimova, Khalilova, 2020].

The goals solved using three-dimensional models include estimation of hydrocarbon reserves, justification of new wells, control over the depletion of reserves at the Hovsan field, assessment of the impact of injection and production wells, and many others [Ahmedov et al., 2018; Salmanov et al., 2023]. Thus, three-dimensional models make it possible to carry out both long-term and operational forecasts when monitoring the development of hydrocarbon deposits.

The Hovsan oil field region's geological and tectonic background. The Hovsan field is located 20 km east of Baku, in the southern coastal part of the Absheron Peninsula. Within the Hovsan area, there are mainly Neogene deposits of the ancient Caspian Sea, rocks of the Absheron and Akchagyl stages, productive strata, and partially Pontus deposits. Miocene rocks lie below the Pontus deposits.

Only the Qala Suite is oil-bearing at the Hovsan field. Lithologically, the Qala Suite is characterized by alternating interbeds of clayey and sandy rocks.

The formation deposits are divided from top to bottom into three sandy-siltstone units: QaS-1, QaS-2, and QaS-3. This division was possible due to the differences in lithology and oil-bearing capacity of the separated strata. Each of the selected layers is subdivided into several smaller layers.

The QaS-3 formation is represented mainly by dark grey dense clays with thinner interlayers of fine and fine-grained sands and dense sandstones. The upper part of the formation contains the largest amount of sand interlayers.

The QaS-2 formation comprises of fine-grained sands with rare interlayers of dense, strongly sandy clays. This part of the section is the most sandy, containing the main oil reserves of the Qala Suite.

The area under study is located within two major structural elements: Kura (northern part of the field) and South Caspian (southern part of the field) depressions. In the south of the area, the South Caspian depression is complicated by the Absheron-Kobustan trough (Fig. 1).

The Hovsan area is part of the East-Absheron synclorium. The distant, eastern dip of the Karachukhur-Zykh anticline hosts the Hovsan area, identified as a weakly pronounced protrusion. The eastern wing of the Karachukhur-Zykh fold, dipping, passes into the Bina-Hovsan syncline, separating it from the Qala fold. The syncline has a south-east-north-west strike and expands towards the Caspian Sea.

Methods. PETREL.10.2 (GeoFrame and Petrel are trademarks of Schlumberger, www.

sis.slb.com; Petrosys Complementing Petrel, <https://www.petrosys.com.au/products-services/petrel/>) software package was used for volumetric modelling of productive formations of the Hovsan oil field. The objects of the study were strata-vault, lithologically screened deposits of productive formations QaS2 and QaS3 of the Qala Suite [Holdaway,

Irving, 2017]. Two 3D-geological models were constructed for the Eastern and Western parts of the Hovsan field. The complex of works covering the whole methodological and technological cycle of geological models construction was implemented following the current RD 153-39-007-96, RD 153-39.0-047-00 and supplementing them «Methodological

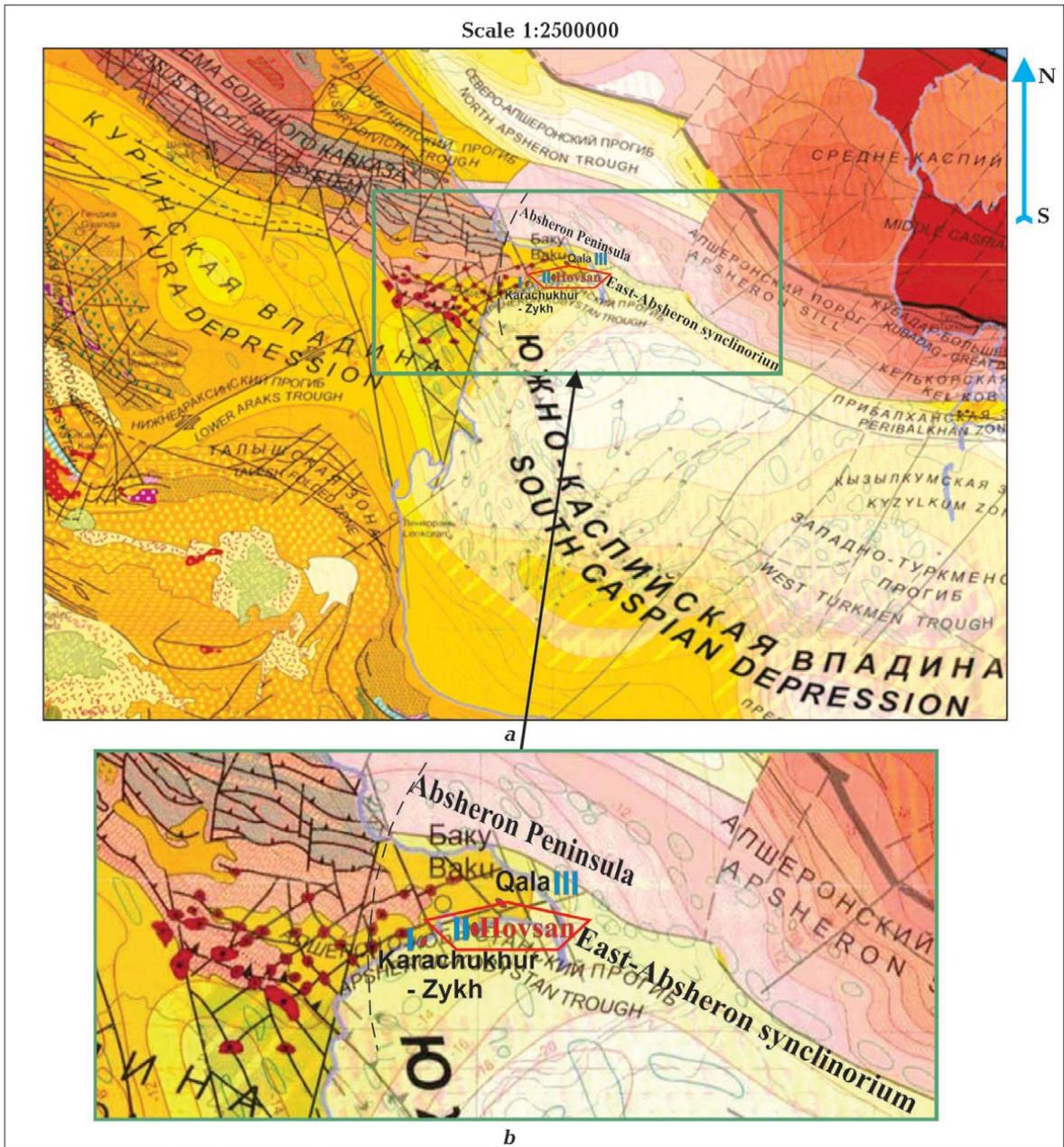


Fig. 1. Tectonic map of the Hovsan area (a), a fragment of the research area of the green part (b) (excerpted from the [Khain et al., 2003]: I — Karachukur-Zykh anticline, II — Bina-Hovsan syncline, III — Qala fold. — contour of works by CDPM (Common Depth Point Method — 3D), — mud diapirs and mud volcanoes, — the same out of scale.

guidelines for the construction of permanent geological and technological models of oil and gas fields», part 1 «Geological models» [Akhmedov, Aghayeva, 2022; Seidov, Khalilova, 2023].

The 3D model construction was carried out in the following sequence:

- 1) Construction of the structural framework for the 3D geological model;
- 2) Quality control, preparation, and loading of source data;
- 3) Construction of a 3D geological model:
 - construction of a 3D geological grid,
 - averaging of borehole data,
 - construction of lithology model (by Simulation method),
 - construction of petrophysical model (by Moving Average method),
 - reserves estimation.

Results. Construction of structural framework for the 3D-geological model. To construct the structural framework for the 3D-geological model, the structural maps for the top and bottom of the QaS2 and QaS3 formations were used. Table 1 shows the structural surfaces forming the structural framework of the 3D geological model [Ahmedov, 2018].

Table 1. Stratigraphic surfaces forming the structural framework of the model

Number	Stratum	Surface
1	QaS2	Top
2	QaS3	Top
3	QaS3	Bottom

Loading source data. The loading of source data consisted of converting the required information into PETREL-compatible formats. The initial digital information for the construction of the geological model of the Hovsan field was [Ahmedov et al., 2023]:

- 80 wells (depths at the top and bottom of formations; inclinometer data: coordinates of wellheads and formation intersections, well trajectory; parametric Well Logging(WL) curves: lithology, saturation character, porosity, oil saturation);
- structural surfaces at the top and bottom of stratigraphic formations;
- lower limit values of porosity and perme-

ability for reservoir rocks, boundary values of oil saturation of reservoirs;

- OWC (Oil Water Contact) levels for wells, the surfaces assumed to be horizontal in the surveyed field.

Quality control of initial data after loading was carried out visually in software complexes developed by «Pangea» JSC and PETREL (Schlumberger). The prepared digital data sets were checked for systematic errors and aligned to create a correct model [Mkinga et al., 2020].

Three-dimensional geological grid. A discrete three-dimensional grid was constructed based on 2D structural surfaces based on stratigraphic marks on the top and bottom of the strata. The grid type is the Corner point, where the cell edges can form arbitrary angles. The Corner point type is the most common grid type at present, as it is more convenient for subsequent hydrodynamic modelling. The vertical structure grid type is proportional (the same number of layers in each grid column) for all modelled reservoirs. This type of grid best describes the geological model. It corresponds to the concept of sedimentation of productive deposits, as well as to the density of drilled wells and seismic survey of the area. Table 2 shows the ranges of thickness variation of a single model layer by strata and the number of model layers, which was selected based on the principle that the maximum height of cells (through which the well passes) in the 3D grid should not exceed 0.4 m.

The 3D grid size of the eastern part of the Hovsan field along the XYZ coordinate axes was 250×330×300 cells (24.750.000 cells). The 3D grid size of the Western part of the Hovsan field along the XYZ coordinate axes was 150×280×300 cells (12.600.000 cells). Spatially, the X axis is directed to the east and the Y axis to the north. The dimensionality of the cells along the lateral of the geological grids is 20×20 m [Kerimova, Khalilova, 2022]. In the 3D grid of the western part of the field, 150 low-volume layers were identified for each layer by the volume of QaS-2 and QaS-3 formations, accordingly. Among these layers, the thickest layer in the QaS-2 formation is 42 cm, the thinnest layer is 13 cm, the thick-

Table 2. To the justification of the number of layers of the 3D grid

Strata	Total formation thickness, m			Accepted number of layers	Thickness of single layer, m		
	Minimum	Maximum	Average		Minimum	Maximum	Average
<i>Western Hovsan</i>							
QaS2	19.5	63.0	48.0	150	0.13	0.42	0.32
QaS3	36.0	79.5	66.0	150	0.24	0.53	0.44
<i>Eastern Hovsan</i>							
QaS2	12.0	72.0	42.0	150	0.08	0.48	0.28
QaS3	18.0	70.0	42.0	150	0.12	0.47	0.28

Table 3. Main geometrical parameters of 3D grids

<i>East Hovsan, basic parameters of 3D grid</i>	
3D grid format	Corner point
Vertical grid type	Proportional
Structural frame	Geological boundaries
Number of Subgrids	2
Spatial dimensions	5.0×6.6 km (in plan), 3770—4720 m (a.m.)
Number of cells	24 750 000
Number of columns (X axis)	250
Number of rows (Y axis)	330
Number of model layers	300
Cell size	20×20 m
<i>Western Hovsan, basic parameters of 3D grid</i>	
3D grid format	Corner point
Vertical grid type	Proportional
Structural frame	Geological boundaries
Number of Subgrids	2
Spatial dimensions	3.0×5.6 km (in plan), 3170—4160 m (a.m.)
Number of cells	12 600 000
Number of columns (X axis)	150
Number of rows (Y axis)	280
Number of model layers	300
Cell size	20×20 m

est layer in the QaS-3 formation is 53 cm, and the thinnest layer is 24 cm. The vertical dimensionality of layers was determined by the total thickness of the layer, the degree of its heterogeneity, the minimum thickness values of permeable and impermeable layers, as well as the number of thin layers. Table 3 shows the main geometrical parameters of the 3D grid.

Well data averaging. The well data contain the following parametric curves required for geological model construction: discrete

lithology curve (reservoir — nonreservoir), discrete saturation curve (0 — nonreservoir, 1 — oil, 3 — water), continuous porosity and oil saturation curves — K_p , K_o . The step of quantization of continuous WL (Well Logging) curves by depth was 0.2 m [Seyidov, Kerimova, 2018; Neamah et al., 2022].

Averaging includes two steps: the determination of grid cells through which the borehole passes and the determination of the weighted average value of the parameter in

each such cell [Shilanov, Tleuzhanov, 2019; Senosy et al., 2020]. After averaging the lithology curve onto the 3D grid, the quality control of the constructions was carried out, and a conclusion was made about the accuracy of the chosen degree of detail of the geological grid. Fig. 2 and 3 show a comparison of the reservoir fraction in the section based on the original parametric las-curves (Log ASCII (digital log curve data) standard) and 3D gridded averaged values of well data (Blocked Wells) for the eastern and western parts, accordingly.

Based on the analysis of Fig. 3, we can say that in the eastern part of QaS-2 formation of the Hovsan field, 69.6 % of layers are non-reservoirs, 19 % are oil reservoirs, and 11.2 % are water reservoirs. The view differs throughout the entire volume of the QaS-3 formation. Thus, 73.5 % of the layers characterizing the formation are non-reservoirs, 15.6 % are oil reservoirs, and 10.7 % are water reservoirs.

Based on the analysis of Fig. 4, in the western part of the QaS-3 formation of the Hovsan field, 56.9 % of the reservoirs are non-reservoirs, 22 % are oil-bearing reservoirs, and 21.1 % are nonreservoirs. 65.1 % of the layers characterizing the QaS-3 reservoir volume are non-reservoirs, 13.9 % are oil reservoirs, and 21.0 % are water reservoirs. Figs. 4 and 5 show histograms of distributions of porosity and oil saturation coefficients on initial parametric data and averaged well data. The main statistical characteristics (minimum, maximum, average values) of both initial and averaged data are also given [Kerimova, 2023b]. According to the analysis of Fig. 5, the maximum value of the porosity coefficient was 25.6 %, and the minimum value was 11.6 % in the whole volume of QaS-2 formation in the eastern part of the Hovsan field. The lowest porosity value in the entire QaS-2 formation is 0.1 % of volume; layers with 18 % porosity represent 22 % of volume, and layers with 25.6 % pro-

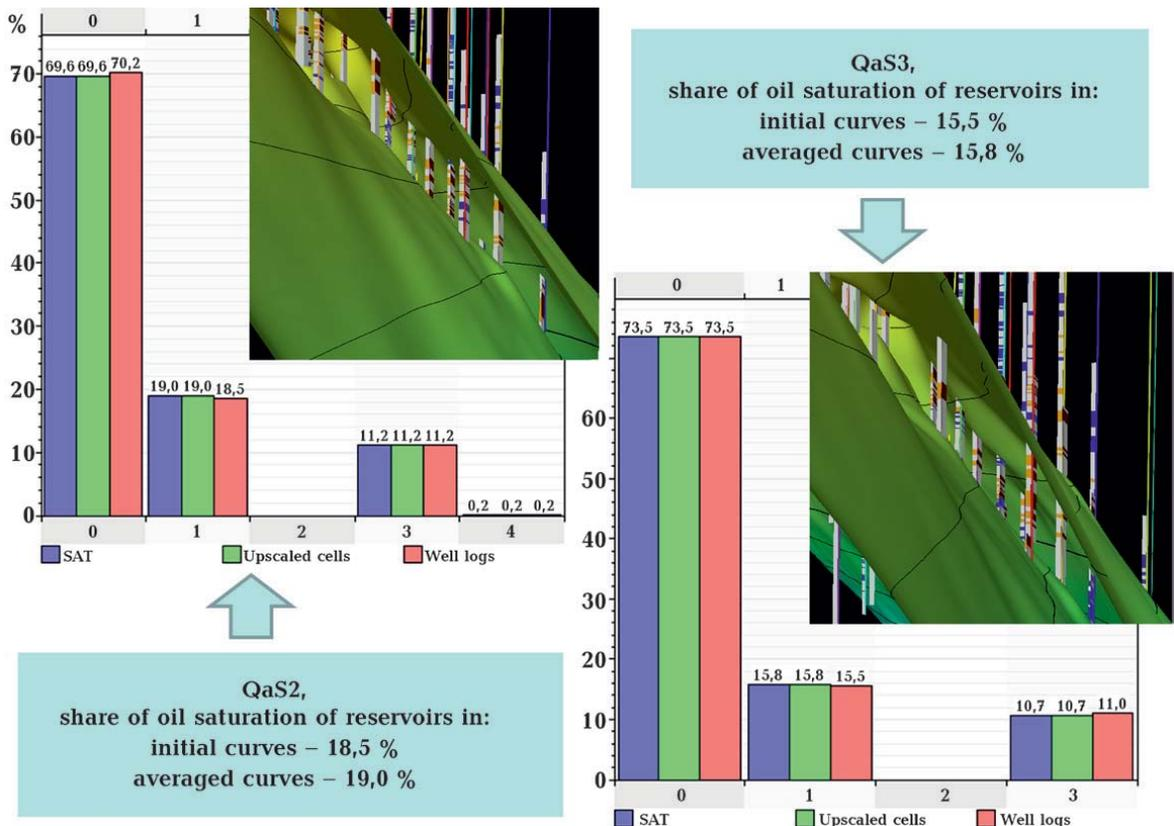


Fig. 2. Comparison of reservoir fraction based on averaged Blocked Wells data (green), saturation (blue), and on the original parametric las-curves (pink) of the Eastern part of the Hovsan field.

sity represent 0.5 % of volume. The maximum value of the porosity coefficient by volume of the QaS-3 formation was 26.4 %, and the minimum value was 12.5 %. In the volume of the QaS-3 formation, layers with the lowest porosity values of 12.5 % represent 1 % of the volume, layers with a porosity of 18.5 % represent 14 % of the volume, and layers with a porosity of 26.4 % represent 1.8 % of the volume.

According to the analysis of Fig. 6, the maximum value of the saturation coefficient was 89.4 %, and the minimum value was 40.5 % for the entire volume of the QaS-2 formation in the eastern part of the Hovsan field. Water reservoirs with $K_o=40\div49$ % in the volume of the QaS-2 formation account for 3.9 % of the volume, oil reservoirs with $K_o=50\div67$ % account for 17.8 % of the volume, and oil reservoirs with $K_o=89.4$ % represent 0.2 % of the volume.

A similar analysis was carried out for for-

mations QaS-2 and QaS-3 in the western part of the Hovsan field. The maximum value of the porosity coefficient by volume of QaS-2 formation was 26.4 %, and the minimum value was 12.1 %. The lowest porosity value of 12.1 % of QaS-2 formation is 3.9 % of the volume, layers with a porosity of 15 % account for 13.9 % of the volume, and layers with a porosity of 26.4 % represent 1.7 % of the volume. The maximum porosity coefficient value was 25.9 %, and the minimum value was 12.1 % for the entire QaS-3 formation volume. By volume of the QaS-3 formation, the layers with the lowest porosity of 12.5 % represent 13 % of the volume, the layers with a porosity of 20 % represent 16.5 % of the volume, and the layers with a porosity of 25.9 % represent 1 % of the volume.

For the QaS-3 formation, the maximum value of the saturation factor was 83 %, and the minimum value was 40.3 %. In the volume of QaS-3 formation, the water-bearing

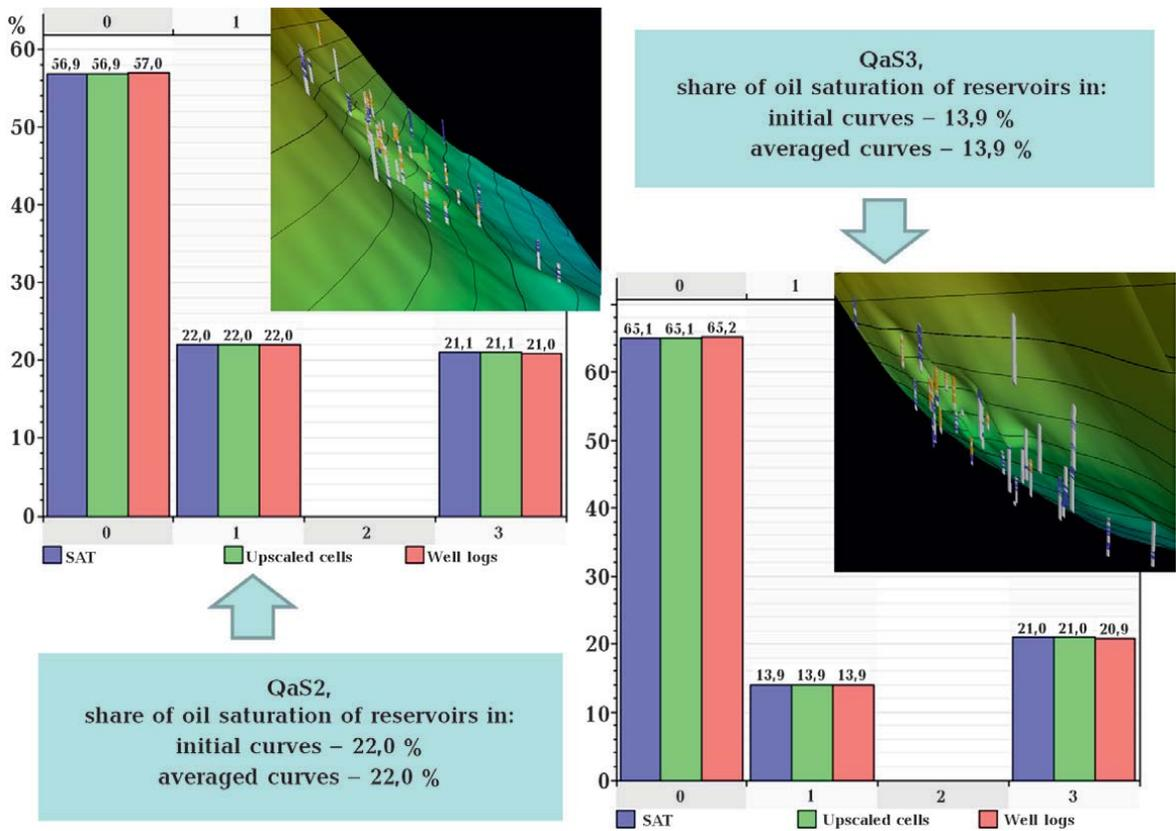
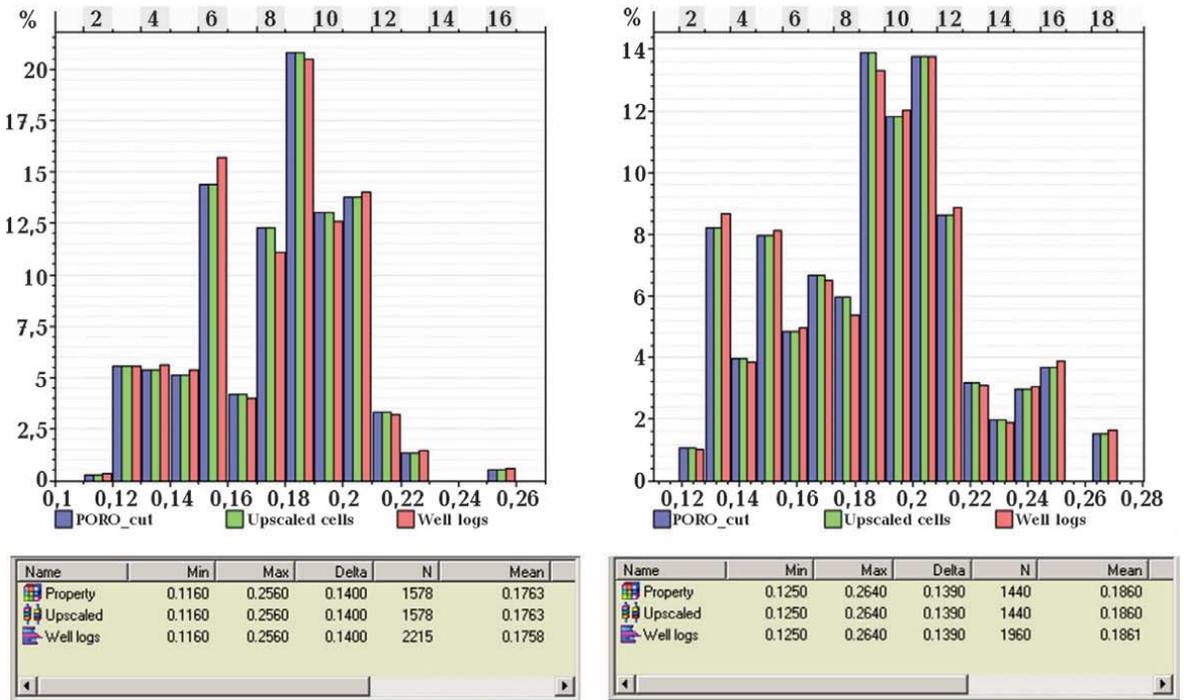
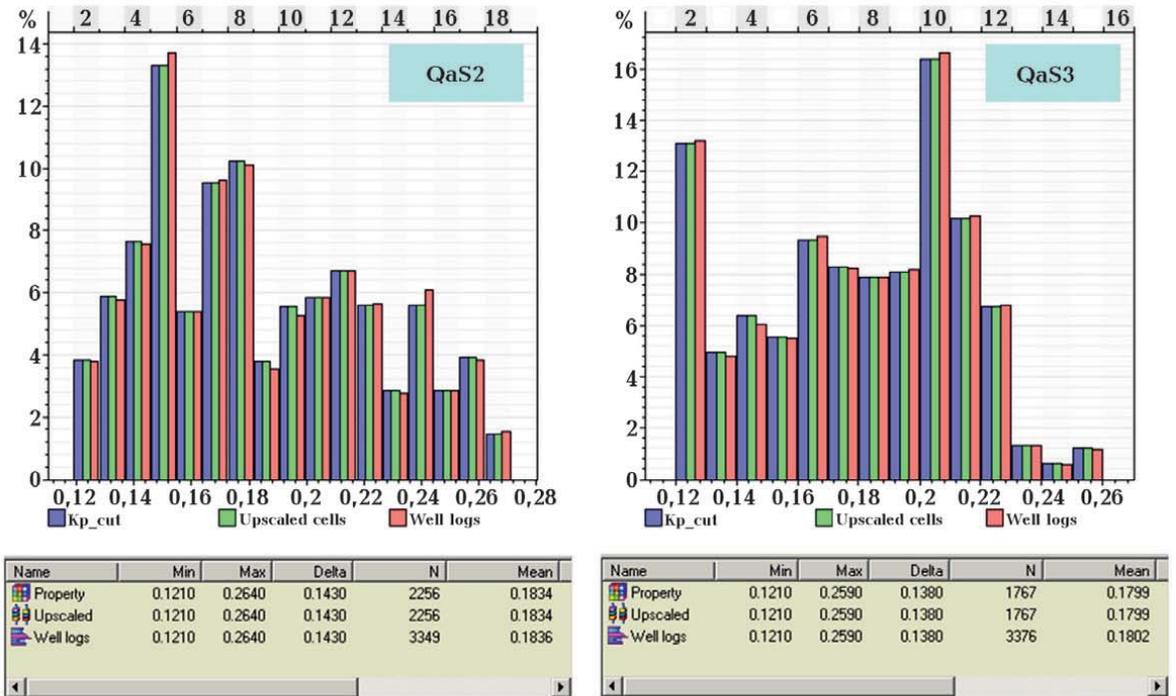


Fig. 3. Comparison of the reservoir fraction based on Blocked Wells averaged data (green), saturation (blue), and original parametric las-curves (pink) of the Western part of the Hovsan field.



Eastern Hovsan



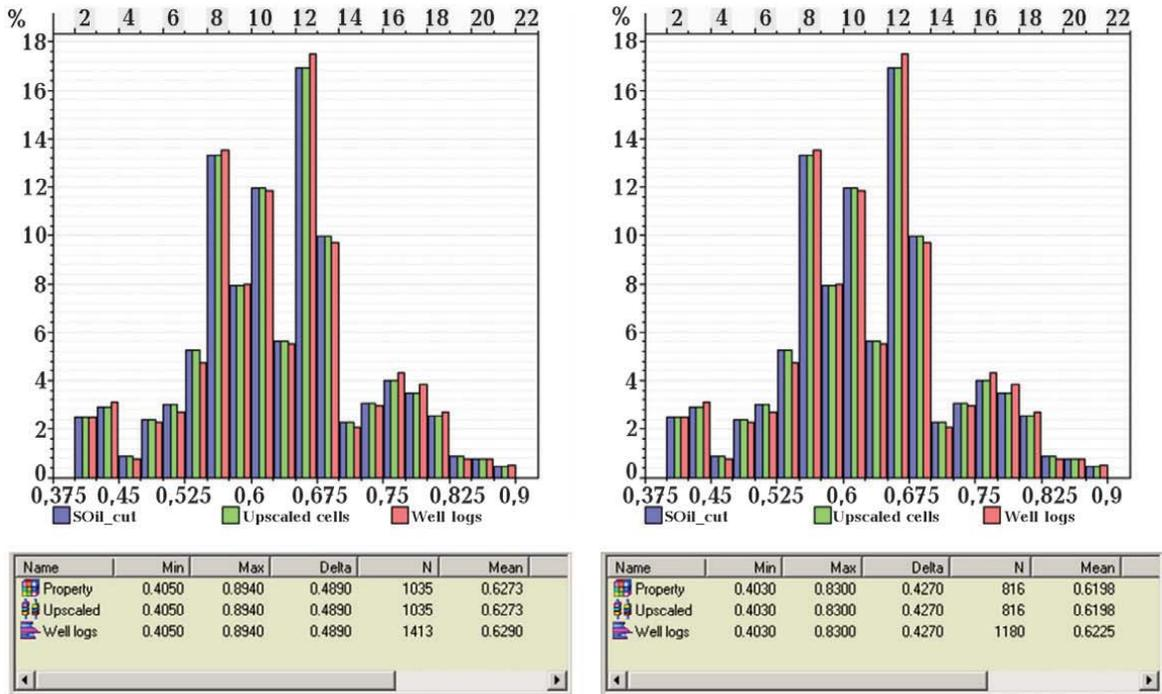
Western Hovsan

Fig. 4. Histograms of porosity coefficient distributions based on initial parametric and averaged well data. Blocked Wells averaged data (green), porosity (blue), and original parametric las-curves (pink).

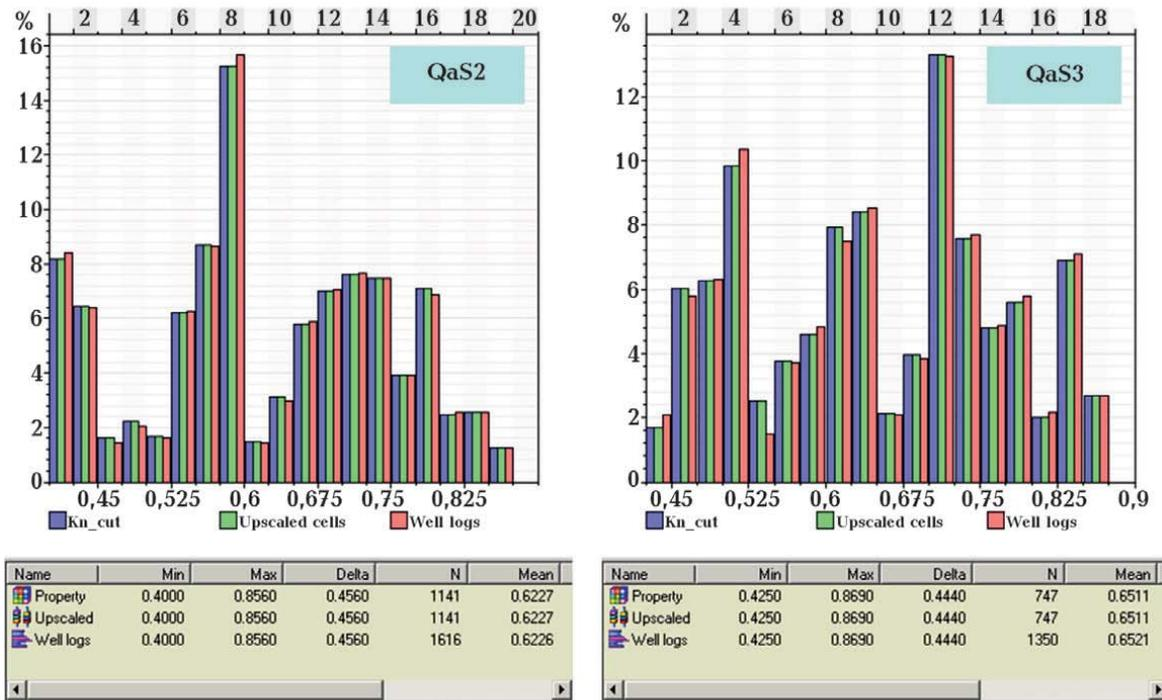
layer with $K_o=40.3\div49\%$ accounts for 3.5 % of the volume, the oil-bearing layers with $K_o=50\div67.5\%$ account for 17.8 % of the vo-

lume, and the oil-bearing layers with $K_o=83\%$ represent 0.2 % of the volume.

A similar analysis was performed for for-



Eastern Hovsan



Western Hovsan

Fig. 5. Histograms of oil saturation coefficient distributions based on original parametric and averaged well data. Blocked Wells averaged data (green), saturation (blue), and original parametric las-curves (pink).

mations QaS-2 and QaS-3 in the western part of the Hovsan field. The maximum value of the saturation coefficient was 85.6 %, and the minimum value was 40 % for the entire vo-

lume of QaS-2 formation of the western part of the Hovsan field. According to the volume of QaS-2 formation, water-bearing layers with $K_0=40\div45$ % account for 8.2 % of the volume,

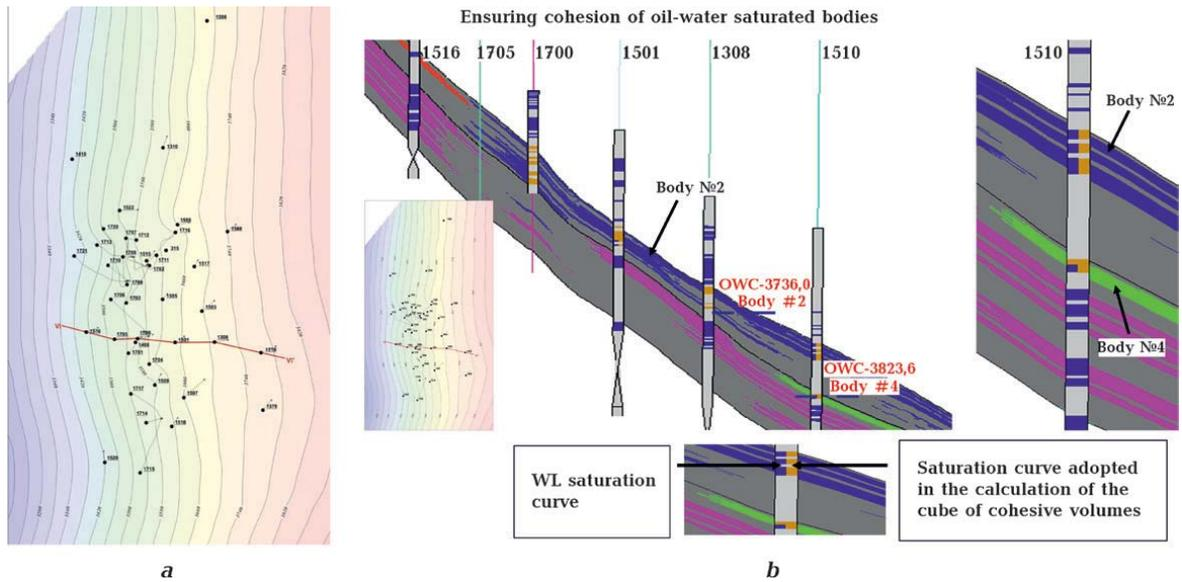


Fig. 6. Structural map showing the location of the investigated wells in the Hovsan field along profile VI—VI' (a). Saturation curve correction for volumetric modelling of lithology. The pink-green (positive values) palette shows oil- and oil-water-saturated (with OWC) sand bodies, and the blue (negative values) palette shows water-saturated sand bodies and gray non reservoirs (b).

water-bearing layers with $K_o=45\div50\%$ account for 2 % of the volume, oil-bearing layers with $K_o=50\div52\%$ account for 1.8 % of the volume, oil-bearing layers with $K_o=55\%$ account for 15.8 % of the volume, oil-bearing layers with $K_o=85.6\%$ account for 2.1 % of the volume.

For the QaS-3 formation, the maximum value of the saturation factor was 86.9 %, and the minimum value was 42.3 %. By volume of QaS-3 formation, water-bearing layers with $K_o=42.5\div49\%$ represent 6.1 % of the volume, oil-bearing with $K_o=50\div52.5\%$ represent 11 % of the volume, oil-bearing with $K_o=70\%$ represent 12.8 % of the volume, oil-bearing layers with $K_o=86.9\%$ represent 2.5 % of the volume.

Lithology model construction. Obtaining the spatial distribution of lithological rock types is one of the most important modelling steps, as three-dimensional fields of reservoir properties and saturation are constructed by considering the lithology parameter. At the lithological modelling stage, each cell must be assigned to a reservoir or non reservoir.

The lithology cube (LITO) is based either on modelling petrophysical properties or on building a cube of the effective thickness

(sandiness) coefficient on the reservoir-not-reservoir parameter and assigning a value of one to cells with a calculated parameter value higher than the boundary value.

There are two common methods of petrophysical modelling: deterministic (Prediction, using interpolation and trending methods) and stochastic (Simulation), used to create equally likely realizations of the spatial distribution of petrophysical reservoir properties.

When creating the lithology cube of the Hovsan field, the geological features of the modelled field were taken into account in the vertical and plan distribution of the reservoir saturation type associated with the lithologically isolated type of deposits and characterized by systematic alternations of water-saturated and oil-saturated reservoirs. Also, certain difficulties in using the results of WL interpretation in lithological modelling are caused by a rather high field depletion, manifested in the nature of saturation of reservoirs in new wells and based on the uplift of the current OWC. This is especially relevant to the western part of the Hovsan field. Taking into account the existing features of the field, some wells were excluded from the modelling of li-

thology and petrophysical properties parameter, and in several wells, the character of well saturation was corrected during modelling.

The following are the steps in constructing the «Lithology» cube.

1. Preparation of Index_SAT lithology curve for modelling sandiness parameter (considering the nature of saturation). Reservoirs with water-saturated reservoirs are assigned index [-1], with oil-saturated reservoir — index [1]. The current indexation allows separating water-saturated bodies from oil-saturated ones based on the results of sandiness parameter construction. However, if the body is two-phase saturated and has an OWC, this approach introduces certain errors when determining the geometry

of bodies in the volume. Therefore, during modelling, reservoirs of wells penetrating a water-saturated reservoir in bodies with OWC are also assigned an index [Kerimova, 2023a]. The saturation character in such bodies was determined after constructing the cohesive volume cube. An example of well saturation pattern curve correction is shown in Fig. 6.

2. Construction of a representative number of 21 realizations of Index_SAT [i] distribution by Sequential indicator simulation (Petrophysical modelling) method. The section on one realization is presented in Fig. 7.

The construction of the AM cube is the average of 21 realizations of the Index_SAT parameter. The section on the AM cube is shown in Fig. 8.

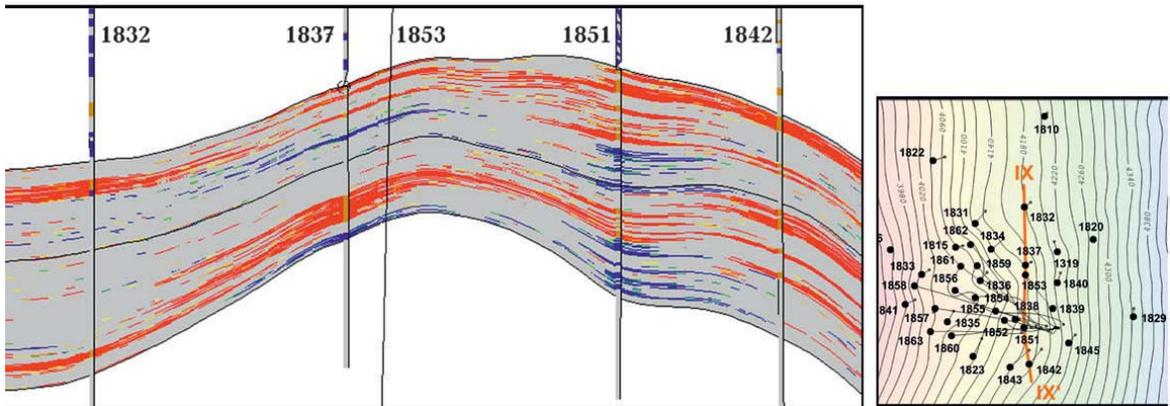


Fig. 7. One of the realizations of the *Index_SAT* parameter distribution. The red (positive values) palette shows oil- and oil-water-saturated (with OWC) sand bodies and the blue (negative values) palette shows water-saturated sand bodies and gray non reservoirs. A structural map showing the location of the investigated wells in the Hovsan field along profile IX—IX'.

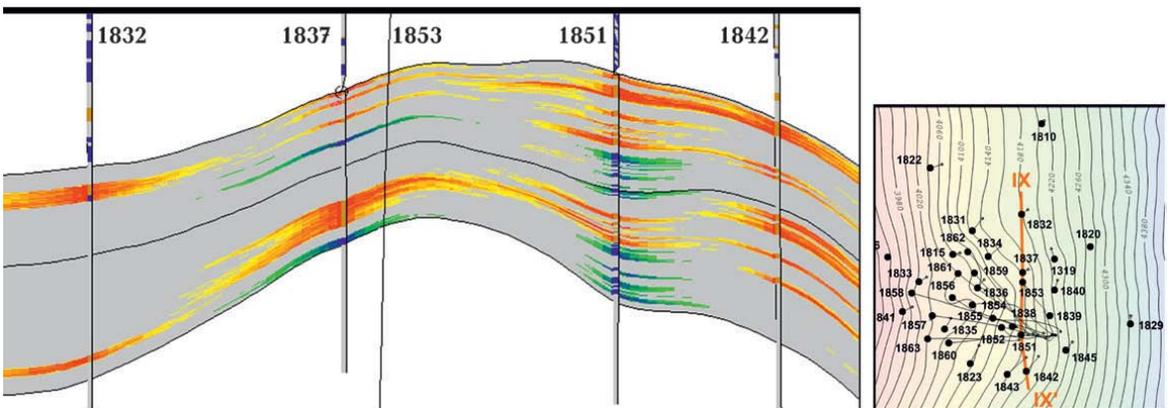


Fig. 8. AM cube section (average of 21 realizations of the *Index_SAT* parameter). The red-yellow (positive values) palette shows oil- and oil-water-saturated (with OWC) sand bodies and the blue-green (negative values) palette shows water-saturated sand bodies and gray nonreservoirs. Structural map showing the location of the investigated wells in the Hovsan field along the profile IX—IX'.

3. Construction of saturation cube. According to the model of the Eastern part of the Hovsan field, AM cube values >0.3 are referred to the oil-saturated reservoir, AM cube values <-0.3 are referred to the water-saturated reservoir, and the rest of the values are referred to non reservoir. In the model of the Western part of the Hovsan field, AM cube values >0.25 are attributed to the oil-saturated reservoir, AM cube values <-0.3 are attributed to the water-saturated reservoir, and the remaining values are attributed to the non reservoir.

When selecting the cutoff, we took into account reservoir connectivity, the consistency of geological and statistical sections (GSS) in the cube and in the original well data, and the behaviour of oil saturated thicknesses in the interwell space. When the cutoff is reduced, false blowups of effective thicknesses begin to appear both between wells and at a certain distance from them. Fig. 9 shows the cross-sections of AM parameter between two wells in the Eastern part of Hovsan field, which

shows unreasonable increase of effective thicknesses in the middle of the distance between wells at a cut-off less than the accepted one, associated with a difficult correlated distribution of reservoir layers in the wells vertically. The increase in effective thicknesses at a cut-off of 0.25 between wells can also be seen on the map.

Fig. 10 shows the GSS (geological and statistical sections) for the oil-saturated reservoir of the Eastern part of the Hovsan field. The GSS is plotted for the zone bounded in the plan by the distribution of oil-saturated bodies. The GSS shows that the share of the oil-saturated reservoir in the cube (shading) is slightly smaller than in the well data (filling).

This discrepancy is explained by several factors: well location in the plan (different drilling pattern) — the extensive water-saturated area is represented by single wells; the need to ensure hydrodynamic separation of water-saturated and oil-saturated bodies; minimizing the increase of unconfirmed thicknesses in the inter-well space.

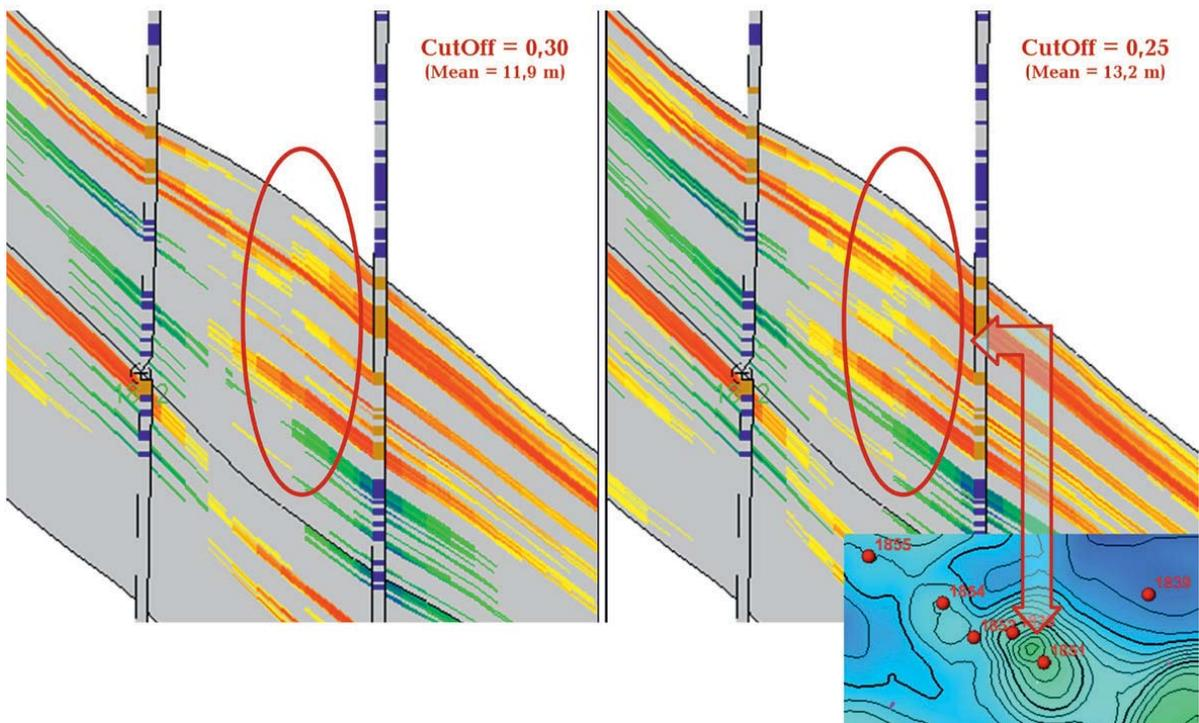


Fig. 9. To select the AM parameter cut-off, false blowups, Eastern Hovsan. The red-yellow (positive values) palette shows oil- and oil-water-saturated (with OWC) sand bodies, and the blue-green (negative values) palette shows water-saturated sand bodies and gray nonreservoirs. A structural map showing the location of the investigated wells in the Hovsan field.

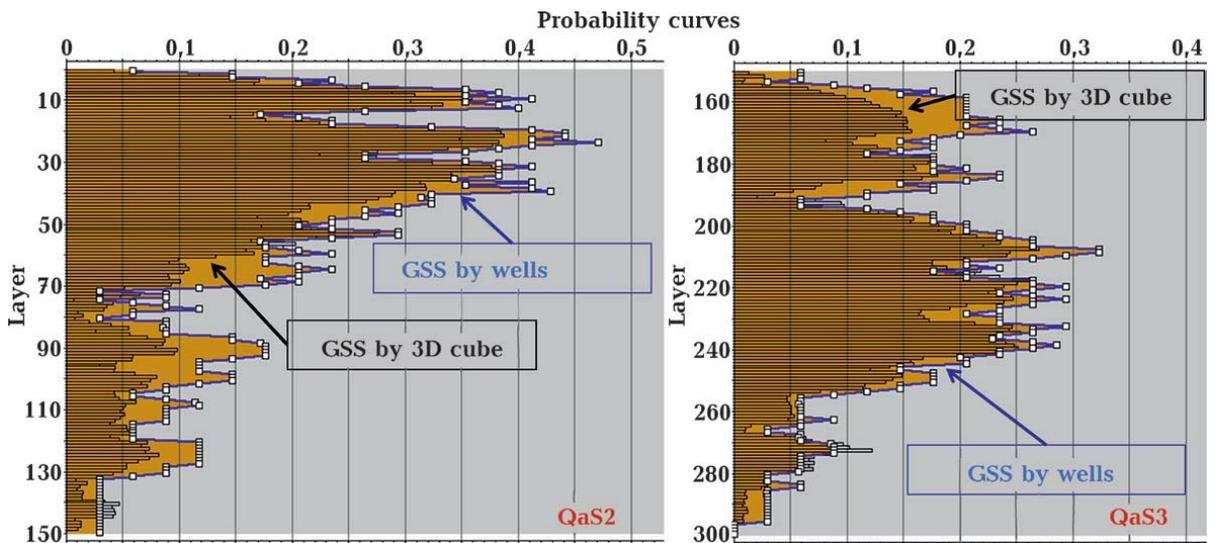


Fig. 10. GSS for oil-saturated reservoirs in the eastern part of Hovsan.

Conclusion. A 3D model of the eastern and western parts of the QaS-2 and QaS-3 formations of the Hovsan field was constructed. Using these models, the formations were separated by reservoir layers, their petrophysical parameters were determined, and their distribution in the field was studied. The oil and gas saturation of these formations was also assessed separately.

References

- Ahmedov, T.R. (2018). The prospective stratigraphic traps of hydrocarbons in the Apsheron suite of seismic data (on the example of the square called «Khasilat» in the south-east of the Apsheron peninsula). *News of the Ural State Mining University*, 1, 18—22. <http://dx.doi.org/10.21440/2307-2091-2018-1-18-22> (in Russian).
- Akhmedov, T.R., & Aghayeva, M.A. (2022). Prediction of petrophysical characteristics of deposits in Kurovdagh field by use of attribute analysis of 3D data. *Geofizicheskiy Zhurnal*, 44(3), 103—112. <https://doi.org/10.24028/gj.v44i3.261976>.
- Ahmedov, T.R., Aliyeva, G.A., & Abdurrahmanova, S.T. (2018). Measurement Geological structure of the Hovsan-Zikh area in the light of 3D seismic survey data for Pontian and Miocene sediments and their oil and gas opportunities. *Vector of Geosciences*, 1(4), 15—27 (in Russian).
- Ahmedov, T.R., Kerimova, K.A., Khalilova, L.N., Alibekova, E.T., Pashayeva, Sh.V., & Aliyeva, G.A. (2023). Building a digital 3D-geological model of the Eastern part of the Hovsan field based on geophysical and geological data. *XII Azerbaijan International Geophysics Conference dedicated to the 100th anniversary of the birth of national leader Heydar Aliyev*. Retrieved from <http://amgk.az/#konferans1> (in Azerbaijani).
- Holdaway, K.R., & Irving, D.H.B. (2017). *Enhance Oil and Gas Exploration with Data-Driven Geophysical and Petrophysical models*. John Wiley & Sons, 368 p.
- Kerimova, K.A. (2023a). Improving the methodology for determining oil saturation of reservoirs using electrical logging. *ANAS Transactions, Earth Sciences*, 1, 60—69. <https://doi.org/10.33677/ggianas20230100094> (in Russian).
- Kerimova, K.A. (2023b). Study of petrophysical parameters of productive series by use of well

- data. *Geofizicheskiy Zhurnal*, 45(3), 135—142. <https://doi.org/10.24028/gj.v45i3.282421>.
- Kerimova, K.A., & Khalilova, L.N. (2022). Delineation of horizons and suites based on quantitative indicators of oil-field geophysical parameters. *Mining Journal*, (12), 4—9. <https://doi.org/10.17580/gzh.2022.12.01> (in Russian).
- Kerimova, K.A., & Khalilova, L.N. (2020). Study of the genesis of deposits of the productive strata based on the data of the logging complex. *Mining Journal*, (8), 68—71. <https://doi.org/10.17580/gzh.2020/08/11> (in Russian).
- Khain, V.E., Bogdanova, N.A. (Eds.). (2003). *International Tectonic Map of the Caspian Sea and its Enclosure. Scale: 1:2500000*. Retrieved from http://neotec.ginras.ru/neomaps/M025_Caspian_2003_Tectonics.jpg.
- Lukin, A.E. (2006). Main regularities of oil and gas deposits formation in the Black Sea region. *Geology and minerals of the World Ocean*, (3), 10—21 (in Russian).
- Mkinga, O.J., Skogen, E., & Kleppe, J. (2020). Petrophysical interpretation in shaly sand formation of a gas field in Tanzania. *Journal of Petroleum Exploration and Production Technology*, (10), 1201—1213. <https://doi.org/10.1007/s13202-019-00819-x>.
- Neamah, A.K., Al-Khafaji, A.J., & Al-Sadooni, F.N. (2022). Evaluation of Petrophysical Characteristics of Mishrif and Yamama Reservoirs, in Garraf Oil Field, Southern Iraq, Based on Well-Logging Interpretation. *Iraqi Journal of Science*, 63(3), 1115—1128. <https://doi.org/10.24996/ij.s.2022.63.3.19>.
- Salmanov, A.M., Maharramov, B.I., & Qaragozov, E.Sh. (2023). *Geology and indicators of oil and gas field development in arid regions of Azerbaijan*. Baku: MSY LLC Publ. House, 624 p. (in Azerbaijani).
- Seyidov, V.M., & Kerimova, K.A. (2018). *Geophysical research methods and interpretation*. Baku, 233 p. (in Azerbaijani).
- Seidov, V.M., & Khalilova, L.N. (2023). Sequence stratigraphic analysis of the Galmaz field based on well logging data. *Journal of Geology, Geography and Geoecology*, 32(2), 360—370. <https://doi.org/10.15421/112333>.
- Senosy, A.H., Ewida, H.F., Soliman, H.A., & Ebraheem, M.O. (2020). Petrophysical analysis of well logs data for identification and characterization of the main reservoir of Al Baraka Oil Field, Komombo Basin, Upper Egypt. *SN Applied Sciences*, 2, 1293. <https://doi.org/10.1007/s42452-020-3100-x>.
- Shilanov, N.S., & Tleuzhanov, A.Z. (2019). Identification of reservoirs and assessment of saturation in conditions of reservoir watering. *Bulletin of the oil and gas industry of Kazakhstan*, 1(1), 48—54.

Тривимірне геологічне моделювання східної та західної частин Говсанського родовища за геолого-геофізичними даними

Т.Р. Ахмедов, К.А. Керімова, Л.Н. Халілова, 2024

Азербайджанський державний університет нафти та промисловості,
Баку, Азербайджан

Розглянуто питання об'ємного моделювання продуктивних пластів нафтового родовища Говсани з використанням програмного пакету PETREL. Як об'єкт дослідження у східній та західній частинах родовища Говсани було взято продуктивні горизонти КаС-2, КаС-3 калинської світи продуктивної товщі. При побудові моделі використовувалися як геологічні, так і геофізичні дані щодо площі досліджень.

На родовищі Говсани промислово значуща нафтоносність у західній і східній частинах, розділених водоносною зоною, пов'язана з відкладами калинської світи

продуктивної товщі. Відклади цієї світи розділені на три горизонти (згори донизу): КаС1 — 57 м, КаС2 — 70 м і КаС3 — 168 м. Загальна потужність калинської світи становить 250 м на західній ділянці та 280 м на східній.

У статті докладно пояснюється методика побудови 3D моделей східної та західної частин родовища Говсани із використанням як геологічних, так і свердловинних даних щодо площі досліджень. Були також включені петрофізична модель східної та західної частин родовища Говсани та літологічний куб для об'ємного моделювання літології.

У статті показано, що піски та пісковики (потужністю 5—15 м), що є нафтогазоносними колекторами, виділяються переважно у верхньому і середньому горизонтах, а також у покривельній частині нижнього шару нижнього горизонту (потужністю 30 м) і чергуються з глинистими прошарками завтовшки 2—3 м. Колекторські властивості шарів змінюються за розрізом і площею.

Хоча родовище Говсани знаходиться в експлуатації більш як 70 років, 3D геолого-геофізичне моделювання було проведено вперше в східній і західній частинах для калинської світи, що вважається перспективною з точки зору продуктивності. Вперше район досліджень детально вивчений з погляду літології, петрофізики та нафтогазоносності міжсвердловинного простору з використанням моделювання на підставі сейсмічних даних 3D. Водночас 3D моделі є основою для вирішення таких питань, як оцінювання запасів вуглеводнів, обґрунтування буріння нових свердловин, моніторинг розробки запасів та оцінювання впливу заводнення та експлуатації добуваних свердловин. Використання тривимірних моделей дало можливість реалізувати як довгострокове, так й оперативне прогнозування при моніторингу експлуатації родовищ вуглеводнів. Оскільки наявність у калинській світі нових об'єктів, які вважаються перспективними з погляду продуктивності, не заперечується їх виявлення та моніторинг із застосуванням тривимірних моделей підтверджені проведеними дослідженнями.

Ключові слова: структурно-параметрична модель, літологічний куб, об'ємне моделювання, петрофізичне моделювання, колектор, пористість, нафтонасиченість.